Linear parametric hydrodynamic models based on numerical wave tank experiments

Josh Davidson
Centre for Ocean Energy Research,
National University of Ireland Maynooth
E-mail: josh.davidson@eeng.nuim.ie

Simone Giorgi
Centre for Ocean Energy Research,
National University of Ireland Maynooth
E-mail: sgiorgi@eeng.nuim.ie

John V. Ringwood
Centre for Ocean Energy Research,
National University of Ireland Maynooth
E-mail: john.ringwood@eeng.nuim.ie

***Abstract*—Hydrodynamic models are important for the design and control of wave energy converters. Traditionally they have been obtained using velocity potential/boundary element type methods, however associated assumptions of inviscid fluid, irrotational flow, small waves and small body motions are a major limitation of this modelling approach, since WECs are designed to operate over wide wave amplitude ranges experiencing large motions, viscous drag and breaking waves. With consideration of the full range of effects, the physics can be described using the Navier-Stokes equations and implemented using computational fluid dynamics (CFD). However, CFD is too computationally expensive for many purposes, for example in initial design optimisation and in the development of control algorithms, where long-time simulations are required. This paper therefore seeks to combine the strengths of both modelling approaches by developing linear parametric models using system identification techniques on CFD generated data. This new approach is demonstrated by identifying the radiation parameters of a linear hydrodynamic model using information from the object's free decay oscillation simulated in a numerical wave tank (NWT). It is shown to have the ability to produce different representative models for different operational amplitudes; an advantage over the traditional approach which is only representative over small amplitude conditions.**

***Index Terms*—Hydrodynamic modelling, system identification, numerical wave tank, CFD, wave energy**

I. Introduction

Hydrodynamic models are used in simulation and control of wave energy converters (WECs). The ability to numerically simulate WEC operation is an essential tool in a WEC developers kit. Estimation of power production, device survivability investigations, parameter optimisation and design of control algorithms are a few examples of where a hydrodynamic model is useful. Through numerical analysis many design configurations can be tested and optimised more easily and cheaply compared to performing the same task experimentally. This is crucial during the early stages of device design, a point recently illuminated by Weber [1] in which he introduced a Technology Performance Level (TPL) metric to be used in conjuction with existing Technology Readiness Level (TRL) metrics which could be used to investigate the optimal development trajectory towards an economically competitive WEC. Analysis of these development trajectories strongly suggests optimising and refining the design to increase its performance ability in the very early design stages through the use of numerical tools.

In the wave energy community, the hydrodynamics are normally formulated under the assumptions of small body motions and wave heights in an incompressible, inviscid and irrotational fluid of constant density. Fully describing the dynamics of the fluid and its interaction with a structure involves solving the Navier-stokes equations, which historically have been simplified to obtain a linear potential flow equivalent whereby solutions are generated by linearising the problem through assumptions of small amplitude oscillations. This is a major limitation of this modelling approach since WECs are designed to operate over a wide range of sea conditions where large amplitude motions will result from energetic waves or sustained wave/WEC resonance. At this amplitude range the linearising assumptions are invalid as nonlinear effects become relevant [7].

For example, in survivability testing simulations the device maybe subjected to waves with a typical 100-year significant wave height of 8 - 13m. In these conditions breaking and overtopping waves will occur and the nonlinear hydrodynamic interaction between waves and the device has a significant effect on the response of the system [7]. Or as another example where wave breaking and overtopping are significant is for the case of a bottom-hinged pitching plate which will experience these effects during regular operation.

With consideration of the full range of effects, the physics can be described using the Navier-Stokes equations. This modelling approach falls into the category of computational fluid dynamics (CFD) and is used in many areas of offshore engineering. CFD is very computationally expensive and not suitable for use in the design process of WECs with regard to efficiency optimisation (through design iterations and development of control algorithms) in real sea states, where long time simulations are required. Therefore, the research in this paper is motivated by the goal of combining the strengths of both modelling approaches; whereby the dynamics of a WEC system can be accurately represented over a wide varying operating range without sacrificing the convenience of the conventional linear model.

Good review of hydrodynamic models include Li and Yu (2012) [7] and Taghipour, Perez and Fossen (2008) [2]. In their systematic review of hydrodynamic modelling methods for point absorber WECs, Li and Yu show that these methods evolved from modelling ship hydrodynamics and offshore

floating structures [7]. At the heart of these modelling methods is the Cummins equation derived in 1962 [5]. There has been plenty of research and progress in this field because of its use in massive industries such as shipping and offshore oil and gas. Hydrodynamic modelling for WECs therefore piggybacks on top of this however is largely still based on linearising assumptions historically necessary for the practical calculation of the problem.

However, Moore's law has continually held since numerical techniques for implementing this research was first conceived. As a result present day researchers are now blessed with the ability to create a NWT in CFD with practical run times. This opens the door for hydrodynamic calculations without the previously required linearising assumptions. Other research groups have also explored the potential of this route. For example the research group in Nantes investigated adding the effect of viscosity to the traditional linear hydrodynamic model from information obtained from CFD experiments [3] [4]. Our contribution is to determine the coefficients of the linear hydrodynamic model from NWT experiments information to yield more representative linear models. These methods have the potential to produce superior results since effects due to viscosity, creation of vorticity in the boundary layer, vortex shedding, turbulence and time-varying wetted body surface area are naturally included.

Layout of the paper. Section II introduces the topic of hydrodynamic modelling by describing the Cummins equation and its implementation using the state space method. Section III describes the commonly used boundary element method of obtaining the hydrodynamic coefficient and shows how these coefficients can be used to determine the parameters of the state space model described in Section II. Section IV then describes a new approach of determining these coefficients using NWT generated data. The results are then presented and discussed in Section V.

II. Linear models for wave energy devices

A. Cummins equation

The Cummins equation forms the basis of hydrodynamic modelling. In 1962, considering the hydrodynamic radiation of a body in an ideal fluid, Cummins [5] showed that for a body with zero-forward speed the linearised pressure induced radiation forces can be expressed as;

$$\mathbf{f}_R(t) = \mathbf{m}_\infty \ddot{y}(t) + \int_{-\infty}^{t} \mathbf{h}_R(t-\tau)\dot{y}(\tau)d\tau. \tag{1}$$

where $y(t)$ is the postion of the body. The first term represents pressure forces due to the accelerations of the body and $\mathbf{m}_\infty$ is the infinite frequency added mass parameter. The second term in this expression relates to the dissipation of energy from the body to the fluid in the form of radiated waves and the term $\mathbf{h}_R(t)$ is the reduced radiation impedence impulse response function.

Adding linearised restoring forces;

$$\mathbf{f}_S(t) = -\mathbf{K}y(t), \tag{2}$$

and considering external waves forces, $\mathbf{f}_e(t)$, leads to the Cummins equation for a body with mass matrix, $\mathbf{M}$;

$$(\mathbf{M} + \mathbf{m}_\infty)\ddot{y}(t) + \int_{-\infty}^{t} \mathbf{h}_R(t-\tau)\dot{y}(\tau)d\tau + \mathbf{K}y(t) = \mathbf{f}_e(t). \tag{3}$$

This represents the general form of Cummins equation for all six degrees of freedom. However to simplify the presentation for the remainder of this paper will only the heave mode of motion shall be explicitly considered. In this mode of motion the restoring force can be derived from hydrostatics in terms of the water density, ρ, gravitational constant, g, and the body's cross sectional area in the free surface plane, S; resulting in the following expression for the Cummins equation describing the heave motion;

$$(M + m_\infty)\ddot{y}(t) + \int_{-\infty}^{t} h_R(t-\tau)\dot{y}(\tau)d\tau + \rho g S y(t) = f_e(t). \tag{4}$$

1) Hydrodynamic information: The geometry of a body influences its interaction with a surrounding fluid and therefore its motion through that fluid. This influence is represented in the Cummins equation through the reduced radiation impedance impulse response function and the infinite frequency added mass terms which contain the hydrodynamic information describing the fluid-structure interaction. These two terms are derived from the hydrodynamic coefficients of the body's radiation impedance, $Z(i\omega)$, which comprises of the radiation resistance, $N(\omega)$ and the added mass, $m_a(\omega)$. At infinite frequency the added mass tends to the finite constant, m_∞, which is subtracted from the radiation impedance to form the reduced radiation impedance, $H_R(i\omega)$ (in order to avoid divergence issues in the radiation convolution integral);

$$H_R(i\omega) = N(\omega) + i\omega\big(m(\omega) - m_\infty\big) \tag{5}$$

The reduced radiation impedance impulse response function can be obtained via the inverse Fourier transform of $H_R(i\omega)$, or directly from $N(\omega)$ with the following relation [6];

$$h_R(t) = \frac{2}{\pi}\int_0^\infty N(\omega)\cos(\omega t)d\omega. \tag{6}$$

These constant hydrodynamic coefficients depend entirely on the body's wetted surface geometry (*As discussed in Section III*) and are commonly calculated only once for a given body, representing its equilibrium position at the still water level. However, once the body and fluid are in motion the wetted surface is dynamically changing, an effect uncaptured by the assumption of constant hydrodynamic coefficients. Additionally, the hydrostatic restoring force co-efficient in the Cummins equation is also constant, which only strictly true in the heave mode for geometries having homoegeneous cross-sections along their vertical axis.

2) Possible extensions: When modelling WECs it is possible to extend Cummins equation. Mooring forces and power take-off (PTO) forces can be included as part of the external force on the right hand side of Equation 4. A common approach to include the viscous drag effect to the non-viscous hydrodynamic forces is to add a quadratic damping term [7] accounting for the effect of viscosity in the same way as in the Morison equation.

B. State-space representation

There are a number of ways to implement the Cummins equation numerically, in the present work the state-space method is used. The convolution integral in the Cummins equation typically makes it difficult to use; however the state space method handles it easily through approximating the convolution integral by a finite-order system of differential equations with constant coefficients. Prony's method finds these coefficients by approximating the impulse response function by a combination of damped complex exponentials. An alternative method, which requires less manual preparations and is also more general, uses a matrix exponential function to approximate the impulse response function [6] [8] and is followed in the present paper.
The convolution integral in the Cummins equation,

$$f_R(t) = \int_{-\infty}^{t} h_R(t-\tau)\dot{y}(\tau)d\tau, \tag{7}$$

can be represented by the following state space sub-system;

$$\dot{\mathbf{x_s}}(t) = \mathbf{A_s}\mathbf{x_s}(t) + \mathbf{B_s}\dot{y}(t), \tag{8}$$

$$f_R(t) = \mathbf{C_s}\mathbf{x_s}(t), \tag{9}$$

where $\mathbf{x_s}(t) = \begin{bmatrix} x_{s1}(t) & x_{s2}(t) & \cdots & x_{sn}(t) \end{bmatrix}^T$ is the state vector. For this state space model to approximate the convolution integral the following must hold [6];

$$h_R(t) = \mathbf{C_s}e^{\mathbf{A_s}t}\mathbf{B_s}, \tag{10}$$

showing how this method uses a matrix exponential function to approximate the impulse response function. There are many possible realisations of the state space model, here the companion-form realisation is used, because it has the advantage of only requiring a small number of parameters [2]. Under this realisation the matrices $\mathbf{A_s}$, $\mathbf{B_s}$ and $\mathbf{C_s}$ are of the form;

$$\mathbf{A_s} = \begin{bmatrix} 0 & 0 & 0 & ... & 0 & -a_1 \\ 1 & 0 & 0 & ... & 0 & -a_2 \\ 0 & 1 & 0 & ... & 0 & -a_3 \\ \vdots & \vdots & \vdots & \ddots & \vdots & \vdots \\ 0 & 0 & 0 & ... & 0 & -a_{n-1} \\ 0 & 0 & 0 & ... & 0 & -a_n \end{bmatrix}, \tag{11}$$

$$\mathbf{B_s} = \begin{bmatrix} b_1 & b_2 & b_3 & ... & b_{n-1} & b_n \end{bmatrix}^T, \tag{12}$$

$$\mathbf{C_s} = \begin{bmatrix} 0 & 0 & 0 & ... & 0 & 1 \end{bmatrix}. \tag{13}$$

Cummins Equation (4), can now be represented by the following state equation;

$$\dot{\mathbf{x}}(t) = \mathbf{A}\mathbf{x}(t) + \mathbf{B}f_e(t), \tag{14}$$

$$y(t) = \mathbf{C}\mathbf{x}(t), \tag{15}$$

where;

$$\mathbf{A} = \begin{bmatrix} 0 & 0 & 0 & ... & 0 & -a_1 & 0 & b_1 \\ 1 & 0 & 0 & ... & 0 & -a_2 & 0 & b_2 \\ 0 & 1 & 0 & ... & 0 & -a_3 & 0 & b_3 \\ \vdots & \vdots & \vdots & \ddots & \vdots & \vdots & \vdots & \vdots \\ 0 & 0 & 0 & ... & 0 & -a_{n-1} & 0 & b_{n-1} \\ 0 & 0 & 0 & ... & 0 & -a_n & 0 & b_n \\ 0 & 0 & 0 & ... & 0 & 0 & 0 & 1 \\ 0 & 0 & 0 & ... & 0 & -\frac{1}{\mu} & -\frac{\rho g S}{\mu} & 0 \end{bmatrix}, \tag{16}$$

$$\mathbf{B} = \begin{bmatrix} 0 & 0 & ... & 0 & 0 & \frac{1}{\mu} \end{bmatrix}^{\mathbf{T}}, \tag{17}$$

$$\mathbf{C} = \begin{bmatrix} 0 & 0 & ... & 0 & 1 & 0 \end{bmatrix}, \tag{18}$$

$$\mathbf{x}(t) = \begin{bmatrix} \mathbf{x_s}(t) & y(t) & \dot{y}(t) \end{bmatrix}^T, \tag{19}$$

here $\mu = (M + m_\infty)$. This linear hydrodynamic model is parameterised by $2n + 1$ parameters $(a_1, ..., a_n, b_1, ..., b_n, m_\infty)$. The next two sections demonstrate two possible methods for identifying these parameters; the first being the traditional boundary element type method and the second being the new approach whereby the parameters are obtained using information from NWT generated data.

III. Determination of the model parameters from the boundary element method

One approach to develop linear hydrodynamic time-domain models consists of using potential theory to compute frequency-dependent coefficients and frequency responses and then use these data to either implement the Cummins equation or to apply system identification to obtain a parametric model that approximates the Cummins equation [9]. This modelling approach is very favourable since it allows obtaining models from limited information about the vessel: hull form and approximate mass distribution [10]. This method is described and implemented in this section using the commercial hydrodynamic software code WAMIT.

A. Hydrodynamic model parameter determination from WAMIT

In section II it has been shown that the convolution term of Cummins Equation (4) can be approximated with a n-subsystem space with 2n parameters $a_1, \ldots, a_n, b_1, \ldots, b_n$ depending on the geometry of the body. The information for this estimation can be obtained from the hydrodynamic parameters in the frequency domain, provided by WAMIT for the utilised body shape, in particular from the radiation resistance $N(\omega)$ utilising equation(6). Once obtained $h_R(t)$, the impulse response curve fitting method [2] is utilised for the state-space model parameter estimation. The approximation of the convolution term is expected to improve increasing the order n of the linear state-space, but an order 2 or 4 is usually good enough [6]. The parameters are estimated such that the impulse response of the sub-system (8) and (9) approximates the impulse response calculated with (6). The fitting error can be calculated with the least-squares [2]:

$$\theta = argmin \sum_i w_i |h_R(t_i) - \hat{h}_R(t_i, \theta)|^2 \qquad (20)$$

where w_i are the weighting coefficients (in the current paper $w_i = 1 \ \forall$ i) and

$$\hat{h}_R(t, \theta) = \hat{C}_s(\theta) exp[\hat{A}_s(\theta) t] \hat{B}_s(\theta) \qquad (21)$$

The above optimization problem is nonlinear in the parameters and we resolved it utilising in Matlab the solver fmincon (based on Hessian calculation). From this optimisation the 2n parameters $a_1, \ldots, a_n, b_1, \ldots, b_n$ are estimated (see figure 1). In the state-space (14) and (15) that approximate the Cummins equation, the last needed unknown parameter m_∞ can be calculated directly from WAMIT (see figure 1). Now that the 2n+1 parameters are estimated a linear model is available to calculate the prediction of the dynamic of the floating body (in the current paper, this identified model is called WAMIT model).

B. WAMIT

The boundary element method, also referred to as the boundary integral equation or panel method, is an advanced potential flow method capable of handling complicated geometries. The wetted surface of the geometry is discretized into panels and the problem is formulated in a boundary integral equation form via Greens theorem whereby the velocity potential throughout the fluid can be represented by surface distributions over the bounding surfaces. By using Dirichlet- and Neumann-type boundary conditions, the potential flow field is calculated by solving the resulting system of linear equations numerically. The pressure on the body surface is then determined from Bernoullis equation and then the forces and moments can be calculated by integrating the pressure over the wetted body surface.
The commercial software package WAMIT implements this type of panel method to calculate hydrodynamic information and has been used in the present paper to provide the hydrodynamic parameters required by the model parameter determination method outlined in this section.

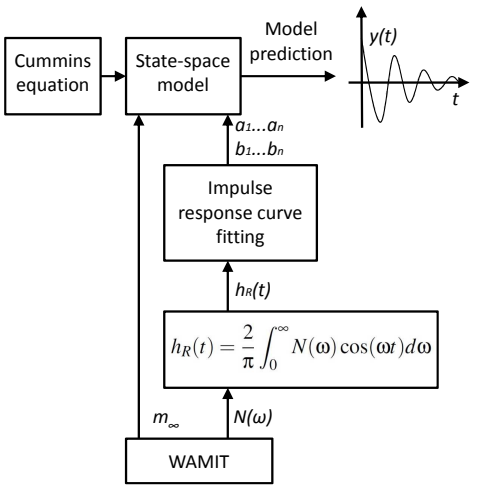

Fig. 1. Block diagram of the sequence of steps to estimate the linear system parameters from WAMIT hydrodynamic parameters.

IV. Determination of the model parameters using numerical wave tank generated data

A. Hydrodynamic model parameter determination from numerical wave tank data

The procedure to utilise NWT data to identify a linear parametric model is based mainly on two steps: a) selection of a set of models (model structure), b) determination of a particular model in the set utilising the information in the data, obtaining in this way specific values for the parameters. The state-space model (14) and (15), obtained from the Cummins equation, can still be utilised for this problem, but in this case it is necessary to find a new strategy to extract information from the NWT data. The step a) and b) are typical objectives in system identification, but it is important to underline that the problem analysed in the current paper presents an important difference with a typical system identification problem, indeed all the numerical experiments simulated in CFD are free decay outputs, based on initial conditions, but without any input force to excite the system. Because system identification is always based on both input-output data , in the current paper the parameter values are estimated resolving an optimization problem. Figure 2 shows the block diagram of the sequence of steps to estimate the linear system parameters from NWT data. The output of the system (14) and (15) is the superimposition of the zero-input component and the zero-state component:

$$y(t) = \mathbf{C} e^{\mathbf{A}(t-t_0)} \mathbf{x}(t_0) + \int_{t_0}^{t} \mathbf{C} e^{\mathbf{A}(t-\tau)} \mathbf{B} f_e(\tau) d\tau \qquad (22)$$

if $t_0 = 0$ and $f_e(t) = 0 \ \forall t$:

$$y(t) = \mathbf{C} e^{\mathbf{A}t} \mathbf{x}(0) \qquad (23)$$

Equation (23) describes the free decay oscillation of the floating body, where $x_{n+1}(0)$ represents the initial displacement of the body from its equilibrium position. The parameters are estimated such that the zero-input response (23) approximates the free decay NWT data. The fitting error can be calculated with the least-squares:

$$\theta = argmin \sum_i w_i |y_{NWT}(t_i) - \hat{y}(t_i, \theta)|^2 \qquad (24)$$

where y_{NWT} are the data generate from NWT and w_i are the weighting coefficients (in the current paper $w_i = 1 \ \forall$ i).
The above optimization problem is nonlinear in the parameters and we resolved it utilising in Matlab the solver fmincon (based on Hessian calculation).
From this optimisation the 2n+1 parameters $a_1, \ldots, a_n, b_1, \ldots, b_n$ and m_∞ are estimated (see figure 2) and a linear model is available to calculate the prediction of the dynamic of the floating body. In the current paper, the identified and utilised models from NWT are called NWT5 model, NWT10 model, NWT25 model and NWT45 model.

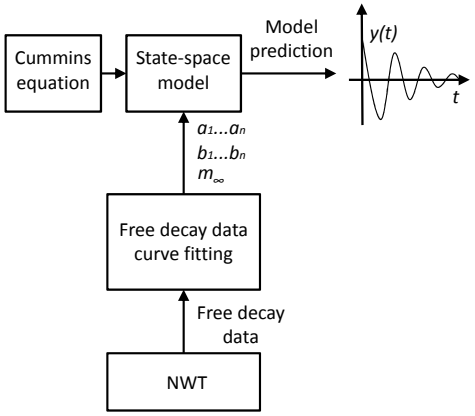

Fig. 2. Block diagram of the sequence of steps to estimate the linear system parameters from NWT data.

B. Numerical wave tank experiments

The type of NWT experiments performed were free decay tests. This involved starting the simulation with the geometry of the body positioned in the middle of the tank with its centre of mass displaced vertically by varying amplitudes from its equilibrium at the still water level (SWL). The simulation is then allowed to run, resulting in free decay body oscillations with a damped sinusoidal profile.

Other possible experiments include creating waves in the NWT and measuring the body response to given input wave signals, analogous to experiments conducted in physical wave tanks with flap or piston type wave makers. An area where a NWT has an advantage over its pyhsical counterpart is the ability to specify and apply any desired external input force profile passively with zero error via a few lines of computer code. The ability to input any force signal, and not one constrained by the physical laws of fluid dynamics e.g. can not have square shaped wave, has advantages in system identification techniques [11]. Such techniques are explored in future work but are outside the scope of the present paper which focuses solely on the case of free decay oscillations in the heave mode of motion.

C. Numerical wave tank implementation

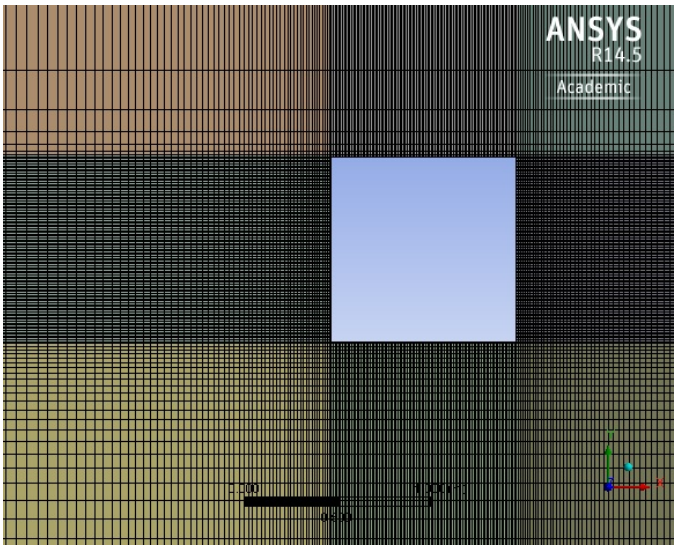

Fig. 3. NWT mesh resolution around the free surface and floating body

The NWT was implemented in the commercial CFD code ANSYS CFX. This CFD software has been used to implement NWTs, notably; Finnegan and Goggins (2012) [12] developed an efficient NWT model in ANSYS-CFX by altering its overall dimensions dependent on the period of the desired deep water waves. In particular the overall height, base length and mesh setup were varied to obtain an efficient model. In his PhD, Maguire [13] researched the hydrodynamics, control and numerical modelling of absorbing wavemakers. A section of his thesis involved a numerical investigation to verify and validate the suitability of ANSYS-CFX to model a physical wavemaker. Silva et al 2010 [14] presented a validation of the commercial code ANSYS-CFX to simulate the generation and propagation of monochromatic waves in intermdiate water. Havn 2011 [15] in his masters thesis investigated the wave forces on the protection covers for submerged offshore pipelines in shallow water, using both a numerical CFD analysis and experiments performed in a physical wave tank. A two dimensional NWT was investigated with ANSYS CFX and then used to study the dynamic wave forces on the protection covers. Shanley et al (2012) [16] implemented a NWT in ANSYS CFX to analyse a novel hull design for an offshore wind farm service vessel.

The length of the tank is 900m and its height is 200m with the bottom 180m filled with water and the top 20m air (both assumed at a temperature of 25C). The tank was made as

long as possible (CFX had an upper bound to the size of the domain) to avoid wave reflections influencing results. The thickness of the NWT is 1cm and symmetry planes are defined as the boundary conditions for the front and back faces thereby transforming the 3D problem into 2D to reduce the required simulation time. The boundary conditions for the two sides and floor of the tank, as well as for the surface of the body, is a no slip wall. The final boundary condition at the top of the tank is an opening.

Figure 3 shows an example of the mesh resolution around the free surface and floating body. Around the still water level the mesh cells have a fine 5mm vertical resolution to accurately capture the free surface. The cells also have 5mm resolution horizontally directly adjacent to the floating body, which is gradually stretched distance away from the body to reduce the number of total cells in the NWT and therefore run time. Stretching the mesh this way has the effect of numerically dissipating the radiative wave by filtering out waves with lengths less than the cell width [13]. In the third dimension the mesh is one cell thick. In total the mesh consisted of 337 000 nodes and 167 000 elements. Temporally the simulation was discretised with a time step of 5ms and had a run time to simulation time ratio of 10^4 using a quad core Intel i7-2600 CPU @ 3.40GHz and 8.00 GB of RAM.

V. RESULTS

The geometry of the body considered in the present analysis is shown in Fig. 4. It has a square face with a side length of 1m and then extrudes 100m orthogonal to this. This geometry was chosen because it could be easily approximated in the 2D NWT, where the symmetry conditions effectively extrude the domain infinitely in the orthogonal direction to the square face. The mass of the body is 49850 kg and the density of the water is specified at 997 kg/m^3, therefore the body sits 50% submerged at equilibrium. The wetted body surface area is illustrated by the shaded region in Fig. 4.

The radiation resistance, $N(\omega)$, was calculated by WAMIT at 180 equally spaced frequencies between 0 and 7.8 rad/s where it converges to zero. It is plotted in Fig. 5.

Four free decay experiments with varying initial displacements were conducted in the NWT. The intitial displacement amplitudes trialled were 5, 10, 25 and 45cm. The results of these simulations are plotted in Fig.6.

A. Model parameter determination

The convolution integral is approximated with a 2nd order state-space subsystem. Therefore there are five unknown parameters to be determined for each model. Table I shows

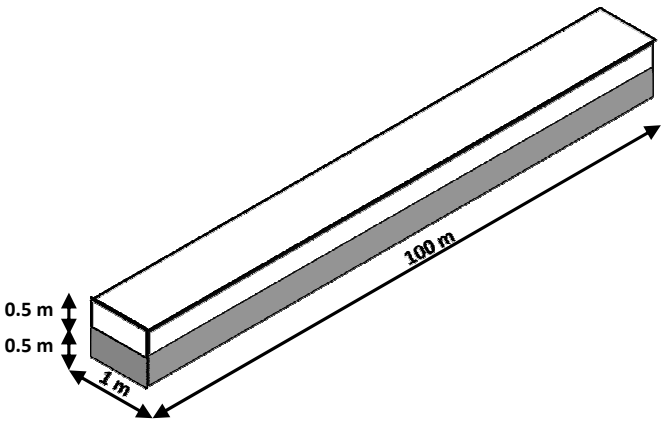

Fig. 4. The geometry of the body used in the present analysis.

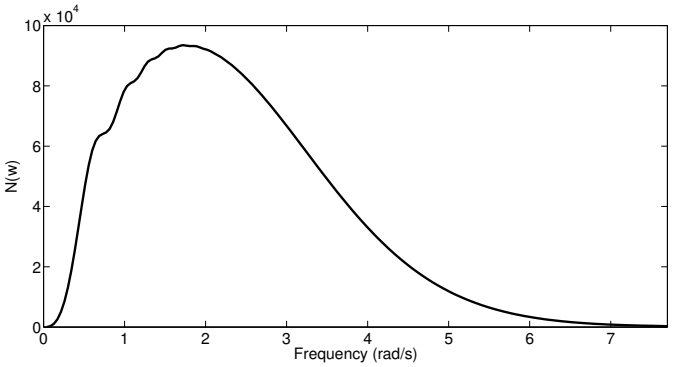

Fig. 5. The radiation resistance for the considered geometry as calculated by WAMIT.

the results determined for these parameters using the methods detailed in Sections III and IV. There are five different models; NWT5, NWT10, NWT25, NWT45 and WAMIT. The model named WAMIT's parameters are determined using the boundary element method and the WAMIT data, and the other four models' parameters are determined using the free decay data sets from the NWT experiments. For these four models, the number in the name represents the initial amplitude of the free decay experiment the model is determined from i.e. NWT25 is the model whose parameters are determined from the NWT

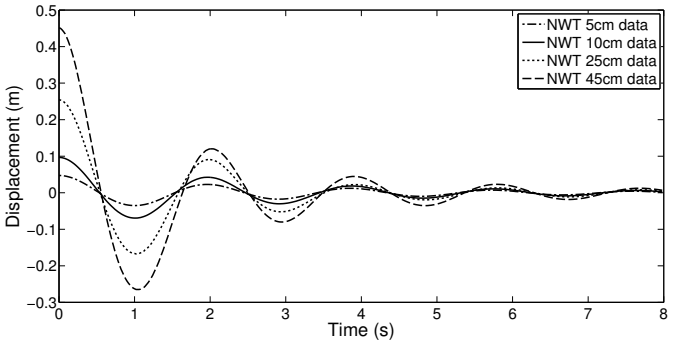

Fig. 6. Simulated results from NWT free decay experiments

Model	$\mathbf{a_1}$	$\mathbf{a_2}$	$\mathbf{b_1}$	$\mathbf{b_2}$	$\mathbf{m_\infty}$
NWT5	4.522	2.988	116400	276100	56280
NWT10	4.664	3.482	123100	339100	56990
NWT25	5.404	4.536	143200	504200	56960
NWT45	3.803	3.783	98250	541000	65380
WAMIT	3.434	2.238	96650	227800	60990

TABLE I
ESTIMATED MODEL PARAMETERS.

Initial amplitude	Fit (%)
5 cm	96.6
10 cm	88.1
25 cm	67.6
45 cm	57.4

TABLE II
THE FIT BETWEEN THE FREE DECAY NWT DATA AND THE PREDICTION FROM NWT5 MODEL WITH INITIAL ELEVATION 5, 10, 25 AND 45 CM.

Initial amplitude	Fit (%)
5 cm	57.4
10 cm	69.3
25 cm	86.5
45 cm	93.8

TABLE III
THE FIT BETWEEN THE 45CM INTIAL AMPLITUDE FREE DECAY NWT DATA AND THE PREDICTION FROM THE FOUR DIFFERENT MODELS WHOSE PARAMETERS WERE ESTIMATED FROM THE 5CM, 10CM, 25CM AND 45CM NWT DATA.

25cm data in Fig.6.

Figure 7 shows the 5cm free decay simulation result from the NWT as well as the predictions obtained by both the WAMIT and NWT5 models when given the same initial condition and zero external input. As to be expected the NWT5 model fits the NWT data very well because it is the exact data set the model's parameters were identified from. This figure also shows the WAMIT model to predict the NWT data reasonably well, a result which could also be expected if the relatively small 5cm intial amplitude of the oscillation satisfies the 'small amplitude' linearising assumptions which WAMIT is based upon.

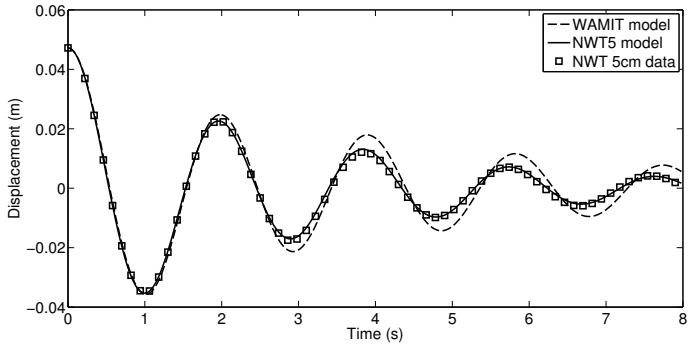

Fig. 7. Plot of NWT simulation result when the body was given an initial displacement of 5 cm. Also plotted the predictions made from WAMIT model and NWT5 model with the same initial displacement. The plot shows the good agreement between the curves.

Increasing the initial amplitude of the free decay experiments is expected to decrease the validity of the linearising small amplitude assumptions. This is illustrated in Fig. 8 where the normalised results of the 10, 25 and 45cm initial amplitude free decay experiments are plotted with the corresponding predictions from the WAMIT and NWT5 models. The first thing to note in this figure is that a linear model's prediction for the three different initial amplitudes reduce to one single line when normalised, a result of linearity. Conversely, the fact that the NWT data varies for different initial amplitudes when normalised illustrates the inherent nonlinearities captured by the CFD simulations. This figure shows a progressive decrease in the accuracy of the two models' predictions as the amplitude increases. This is also shown objectively by using the Fit as a metric for comparison in Table II. The Fit between two curves is defined as:

$$Fit = 100\Big(1 - \frac{\|y_{data} - y_{pred}\|_2}{\|y_{data} - \overline{y_{data}}\|_2}\Big) \qquad (25)$$

where $\|x\|_2 = \big(\sum_i |x_i|^2\big)^{1/2}$, y_{data} is a data generated from NWT, y_{pred} is a prediction from an identified model and $\overline{y_{data}}$ is the average value of y_{data}.

This illustrates the non-linearity of the floating body's dynamics in that one linear model is not representative over the entire operating region of the system. To further investigate this, the five different models are used to predict the free decay response from an intial amplitude of 45cm. These predictions are compared against the actual 45cm free decay experiment data from the NWT in the graph in Fig. 9. In this figure it is possible to see that the predictions are worse for the models whose parameters are determined from the smaller amplitude initial conditions. This is also shown objectively by using the Fit as a metric for comparison in Table III. Figure

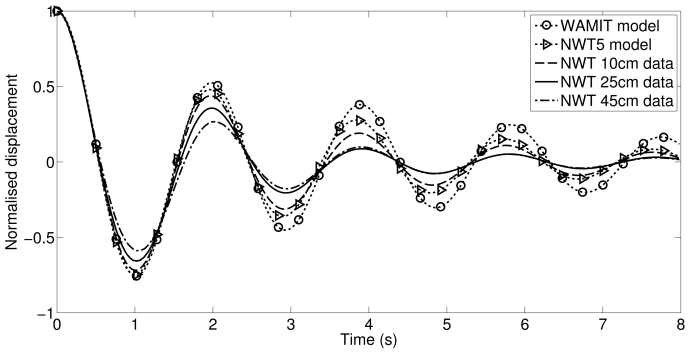

Fig. 8. Normalised displacements: plots of NWT simulations with initial displacement of 10cm, 25 cm and 45cm. Also plotted the predictions made form WAMIT model and NWT5 model for the same initial displacement.

8 showed that the damping profile is greater for the larger initial amplitude oscillations. This effect can be investigated by calculating the position of the poles of mode. Figure 10 shows that each model has two pairs of complex conjugate poles. For a linear system, its dominant poles are the most important to describe its dynamics and the larger their negative real value

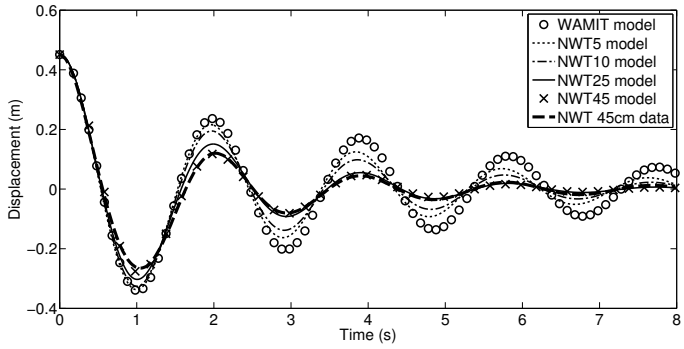

Fig. 9. Plot of predictions made from WAMIT model, NWT5 model, NWT10 model, NWT25 model, NWT45 model for the same initial displacement 45cm. Also plotted the NWT simulations with initial displacement of 45cm.

the greater the damping effect (the oscillations decay faster). This figure shows that the models whose parameters are determined from the larger initial amplitude conditions indeed do have larger damping profiles than for models determined from the smaller amplitude conditions. The arrows in figure 10 show this trend.

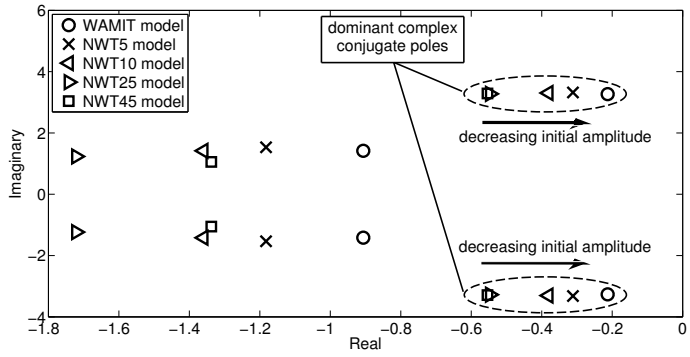

Fig. 10. Poles location of the identified WAMIT model, NWT5 model, NWT10 model, NWT25 model and NWT45 model.

The results in this section indicate that different linear models are required to represent different operating amplitudes. Since NWT data can be simulated for different operating regions, this gives the present method an advantage over WAMIT as WAMIT only gives parameters valid only for very small operating condition. The ability to develop different linear models locally representative of different operating regions opens the door for non-linear modelling approaches which switch between different representative linear models at the different operating points.

VI. Conclusion

Linear hydrodynamic models are important in the design, simulation and control of WECs. In this paper a new approach to determine the parameters of a linear hydrodynamic model is outlined whereby the parameters are identified from information generated using CFD simulations rather than from traditional velocity potential / boundary element generated hydrodynamic data. The simulated responses from NWT experiments designed to excite the relevant dynamics of a floating WEC can be used by system identification techniques to identify the parameters of a linear hydrodynamic model representative of the observed dynamics. In this way the information used to determine the model parameters implicitly contains the full range of effects described by the Navier-Stokes equations many of which have been traditionally neglected or linearised by velocity potential / boundary element techniques.

An example of this approach is shown by providing a Cummin's representation of a heaving rectangular barge through the identification of heave decay tests obtained with a commercial CFD software. From this example it is shown that determining the parameters of a linear hydrodynamic model using data generated from NWT experiments allows different representative models to be determined for different operating amplitudes, which is not possible using traditional methods based on information obtained from linear velocity potential / boundary element methods.

References

[1] J. Weber, "Wec technology readiness and performance matrix–finding the best research technology development trajectory," in *International Conference on Ocean Energy, Dublin, Ireland*, 2012.

[2] R. Taghipour, T. Perez, and T. Moan, "Hybrid frequency–time domain models for dynamic response analysis of marine structures," *Ocean Engineering*, vol. 35, pp. 685–705, 2008.

[3] M. Bhinder, A. Babarit, L. Gentaz, and P. Ferrant, "Effect of viscous forces on the performance of a surging wave energy converter," in *Proceedings of the Twenty-second (2012) International Offshore and Polar Engineering Conference*, 2012.

[4] ——, "Assessment of viscous damping via 3d-cfd modelling of a floating wave energy device," in *European Wave and Tidal Energy Conference (EWTEC 2011)*, 2011.

[5] W. Cummins, "The impulse response function and ship motions," DTIC Document, Tech. Rep., 1962.

[6] Z. Yu and J. Falnes, "State-space modelling of a vertical cylinder in heave," *Applied Ocean Research*, vol. 17, pp. 265–275, 1995.

[7] Y. Li and Y. Yu, "A synthesis of numerical methods for modeling wave energy converter - point absorbers," *Renewable and Sustainable Energy Reviews*, vol. 16, pp. 4352–4364, 2012.

[8] Y. Zhi and J. Falnes, "State-space modelling of dynamic systems in ocean engineering," *Journal of Hydrodynamics, Ser. B*, vol. 1, pp. 1–17, 1998.

[9] T. Perez and T. I. Fossen, "Practical aspects of frequency-domain identification of dynamic models of marine structures from hydrodynamic data," *Ocean Engineering*, vol. 38, pp. 426–435, 2011.

[10] T. Perez and T. Fossen, "A derivation of high-frequency asymptotic values of 3d added mass and damping based on properties of the cummins equation," *Journal of Maritime Research*, vol. 5, pp. 65–78, 2008.

[11] L. Ljung, *System identification*. Wiley Online Library, 1999.

[12] W. Finnegan and J. Goggins, "Numerical simulation of linear water waves and wave-structure interaction," *Ocean Engineering*, vol. 43, 2012.

[13] A. E. Maguire, "Hydrodynamics, control and numerical modelling of absorbing wavemakers," Ph.D. dissertation, The University of Edinburgh, 2011.

[14] M. C. Silva, M. de Araujo Vitola, W. T. Pinto, and C. A. Levi, "Numerical simulation of monochromatic wave generated in laboratory: Validation of a CFD code." in *23 Congresso Nacional de Transporte Aquavirio, Construo Naval e Offshore*, 2010.

[15] J. Havn, "Wave loads on underwater protection covers," Master's thesis, Dept of Marine Technology, NTNU, 2011.

[16] M. Shanley, J. Murphy, and P. Molloy, "Offshore wind farm service vessel, hull design optimisation," in *International Conference on Ocean Energy (ICOE 2012)*, 2012.